Report to the RHIC Spin Collaboration Annual Meeting
MIT, Cambridge, MA, 7-8 May, 1995

STAR Note #237
January 31, 1996

STAR SVT in High Luminosity pp Collisions at RHIC

(How Useful Is the SVT for Doing Spin Physics in STAR)

V. L. Rykov[1]

For the STAR SVT Collaboration

Department of Physics and Astronomy, Wayne State University,
Detroit, Michigan 48202, USA

Abstract.

The enhancement of STAR's capability to select triggered events at high luminosity using the Silicon Vertex Tracker has been studied. The impact of the SVT on vertex reconstruction and high P_T momentum resolution in STAR is also discussed.

[1]Visitor from the Institute of High Energy Physics, Protvino, Moscow District 142284, Russia.

Introduction

The STAR Silicon Vertex Tracker (SVT) [1] is a subdetector which can significantly enrich STAR's potential for doing spin physics at RHIC [2]. However, until now it did not receive enough attention to reveal all of its unique powers either for studying specific processes (production of short-living particles in polarized proton collisions, etc), or to enhance the capabilities to carry out high precision spin physics in general. For example, the vertex position and momentum resolutions for charged particles with the SVT are significantly better than with only the Time Projection Chamber (TPC) due to the SVT's high spatial resolution and its location close to the beam. Also, the SVT can help considerably in the selection of triggered events when RHIC operates at high luminosity, up to $2 \cdot 10^{32}\,cm^{-2}s^{-1}$. Operating at high luminosity is a serious problem in STAR because its main tracker, the TPC, is extremely slow, and the tracks from the triggered event will coexist in the TPC's sensitive volume with the tracks of events from the hundreds of bunch-crossings preceding and following the trigger. The improvement of event selection as well as the momentum and vertex position resolutions are important for the reduction of the background in the reactions which are to be studied in STAR with polarized protons.

In this report we will concentrate on the latter issues, namely, how the SVT can be used to select the triggered event and how it improves vertex position and high P_T momentum resolutions in STAR.

1 SVT Setup

The STAR SVT (Fig. 1a) will use 216 $6.3 \times 6.3\,cm^2$ Silicon Drift Detectors (SDD) [3] in three concentric barrels designed to cover the angular range from $\sim$$-45^o$ to $+45^o$ in θ and 2π in azimuth, φ. Each barrel consists of 8, 12, or 16 ladders, each holding 4, 6, or 7 wafers, resulting in three SVT layers of total lengths 25, 38, and 44 cm respectively. Due to construction requirements, even the ladders in a single barrel are not all located at the same distance from the beam line, but are grouped around the radii of 6.5, 10.5 and 14.4 cm from the beam.

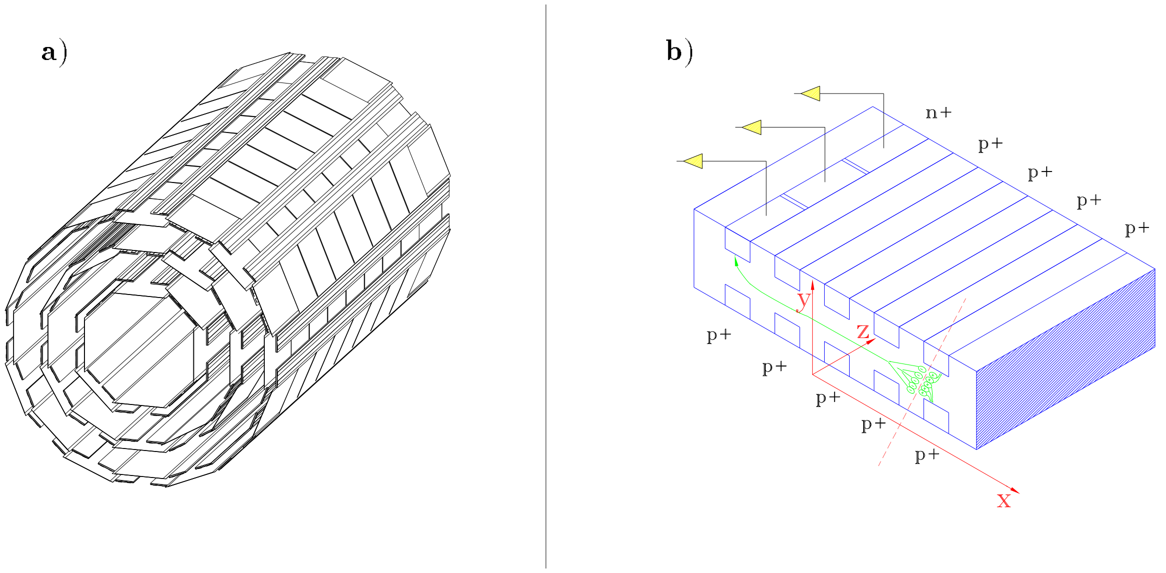

Figure 1: STAR SVT (**a**) and the schematic picture of the SDD (**b**).

The two-dimensional position of a particle hit in the SDD is measured in the following way (see SDD schematic view in Fig. 1b). After the passage of an ionizing particle through the SDD, the created electron cloud is immediately (in ∼5–10 ns) confined to a "pancake" with the thickness of ∼10–20 μm (∼3–7% of the total SDD thickness of 300 μm) to the SDD mid-plane. At the same time, the cloud starts to drift along the x–axis in the uniform electric field applied to the SDD, with a constant velocity $V_{drift} \simeq 6.4\ \mu m/ns$. The electron cloud eventually arrives at the anodes located at the SDD edge, generating signals in the corresponding channels. By measuring the time delay between the trigger and the signal's appearance, the x position of the hit can be determined with a resolution (RMS) of $\sigma_x \simeq 20$–$25\ \mu m$ [1, 4, 5, 6]. In the STAR global frame of reference, the drift in the SDDs occurs in the azimuthal direction.

The SDD anode is divided into 240 separate pieces with the width of the charge collecting area equal to 250 μm for each channel. The position of the particle hit along the z-axis (along the beam line) can be determined by the position of the anodes where the electron cloud arrives. An electron cloud, when drifting in the SDD mid-plane, expands rapidly to a size (RMS) of ∼100–200 μm due to electron diffusion and Coulomb repulsion. Therefore, the signals are generated at several adjacent anodes rather than at a single one. As a result, the reconstruction accuracy, σ_z, of the z position derived as a weighted average of the signals in adjacent anodes for the drift distances ≥1–2 mm, is on the order of 20–25 μm, same as for $\sigma_x \equiv \sigma_\varphi$.

The anodes of each wafer ("double-SDD")[2] are located along the two opposite edges of the active area at $x = \pm 30$ mm (in the local frame of the Si wafer), but the high voltage creating the drift field is applied along the line $x = 0$. So, the drift in the two wafer halves occurs in opposite directions. The maximum drift length in the SDD is equal to 30 mm, and the maximum drift time is ≃4.7 μs, about 8–10 times smaller than the TPC drift time.

2 Acceptance and Detecting Efficiency

Unlike the STAR TPC or Electromagnetic Calorimeter (EMC), it would be incorrect to point out some single number for the SVT acceptance in η because, due to the SVT's close location to the beam line, its acceptance quite strongly depends on the vertex location within a collision "diamond"[3] of the length $\sim \pm 5\,cm$. The dependence of the SVT acceptance in η on the vertex location is shown in Fig. 2. One can observe that, at least for $\mid z_{vertex} \mid \leq 5\,cm$ where ∼68% of the events will occur, the central region of $\mid \eta \mid \leq 1$ is covered by all three SVT layers. For most of the remaining events, the swing, $\eta_{max} - \eta_{min}$, remains ∼2 while the central point, $(\eta_{max} + \eta_{min})/2$, is located within the interval from zero to ∼1/2.

The SDD detection efficiency within its active area is very close to 100%. However, each wafer has a high voltage guard area which is insensitive to the ionization. These areas occupy ∼4.5% of the total SVT coverage. As a result, for a track crossing all three SVT layers, the probability for all three hits to be detected is $\sim(0.955)^3 \simeq 87\%$. The probability for a track to be detected at least in two layers is ∼99.4%, and it is ∼99.99% for at least one hit.

[2] To avoid confusion, in the rest of this paper the term "SDD" is applied to half of the "double-SDD" which, in turn, denotes the Si wafer of the size 6.3×6.3 cm^2. A wafer consists of two SDDs, drifting in the opposite directions, and also include the high voltage guard area.

[3] In pp mode, the events will have a Gaussian distribution within the collision diamond:

$$\frac{d^2 N_{event}}{dr\,dz} \propto \frac{r}{\sqrt{2\pi}\sigma_{rd}^2 \sigma_{zd}} \cdot \exp\left(-\frac{r^2}{2\sigma_{rd}^2} - \frac{z^2}{2\sigma_{zd}^2}\right)$$

with widths $\sigma_{rd} \simeq 96\ \mu m$ and $\sigma_{zd} \simeq 5.1$ cm [7].

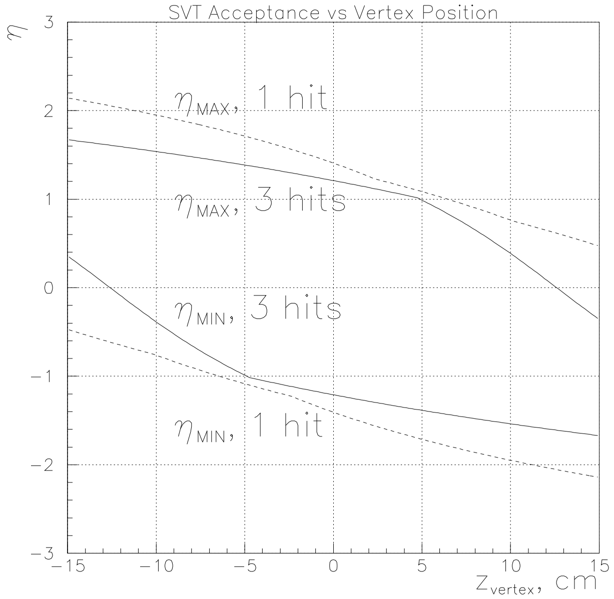

Figure 2: SVT η-acceptance. Solid lines are for the three-hit acceptance and dashed lines are for at least one hit in any SVT layer.

3 Detector Occupancy

The STAR experiment was originally designed for high multiplicity events but low event rates from heavy ion collisions. Both its tracking detectors, SVT and TPC, are pixel-structured but have the memory times of ~4–5 μs (SVT) and 40–50 μs (TPC). In the high luminosity pp mode, the situation is very different from that in heavy ion collisions. The multiplicity in a single pp event is relatively low, but the rate of background minimum bias events is expected to be very high, up to $\sim 10^7$ Hz. The result is that the total occupancy will comprise the tracks from the triggered event and also the tracks from tens or even hundreds of background events which must be rejected.

The multiplicity of charged particles in the triggered event depends on the type of the event. The main focus of the spin program at RHIC is the study of hard parton collisions: production of high-P_T jets, direct photons, $W^{\pm}$, Z^0, etc [2]. The multiplicities for some processes of interest, obtained by simulations with *PYTHIA/JETSET* event generator, are shown in Table 1.

Table 1: Multiplicity of charged particles, $<N_{ch}>$, in pp collisions at $\sqrt{s} =$ 500 GeV within $|\eta| \leq 1$.

Process	$<N_{ch}>$, All P_T	$<N_{ch}>$, $P_T > 0.5\,GeV/c$
Jets, $P_T^{jet} > 20\,GeV/c$	~20	~13
Direct γ, $P_T^{\gamma} > 10\,GeV/c$	~12	~6
$pp \to W^{\pm} + X \to e\nu + X$	~7.5	~3
$pp \to Z^0 + X \to e^+e^- + X$	~7.5	~3
Minimum bias	~3.5	~1

The estimated [8] total pp cross-section at $\sqrt{s} = 500$ GeV is ~60 mb. Thus, ~100–120 minimum bias events will occur during the SVT readout time at the luminosity of $2 \cdot 10^{32}\ cm^{-2}\,s^{-1}$, but approximately ten times more events will occur during the TPC readout. For minimum bias events (including pp elastic scattering), the average multiplicity of charged particles is ~3–4 tracks/event within $\Delta\eta \simeq 2$. Approximately half of the background hits in each TPC and SVT layer will either drift out of the sensitive volume/areas before the readout starts, or will arrive at the anodes after the readout ends. As a result, ~2,000–4,000 hits in each TPC row will be read out by the Data Acquisition System (DAQ), i.e. the TPC occupancy in *pp* mode will be about the same as in heavy ion collisions [1]. In the SVT, due to the shorter drift time, the occupancy will be ~200–300 hits/layer, ~10 times less than in a central Au-Au event. This corresponds to a hit density of 4–5 per SDD (area 6×3 cm^2) in the inner SVT layer, and ~1 hit/SDD in the outer layer. Such densities do not seem too high for the pixel structure with a pixel size of ~250×250 μm^2. Typical pictures of an SVT section with the hits from the triggered jet and 120 minimum bias events are shown in Figs. 3–6a[4].

4 Direct High-P_T Track and Vertex Finding

The first step in selecting the triggered event is to find as many of the tracks which emerge directly from its vertex as possible. The first candidates to look for are the "high-P_T" primary charged particles whose tracks are easy to recognize because of their low curvature. A threshold, P_T^{min}, has to be introduced to define all tracks with $P_T \geq P_T^{min}$ as the "high-P_T" ones. On one hand, this threshold has to be high enough so that high-P_T tracks will be close to straight lines; on the other hand, the threshold should not be too high or we will not have enough high-P_T tracks in the triggered event for unambiguous recognition and reconstruction of the vertex these tracks have emerged from. For the processes listed in Table 1, a threshold of ~0.4–0.5 GeV/c seems reasonable because ~50% of direct particles in these reactions have $P_T \geq 0.5$ GeV/c. At the same time, these tracks are nearly straight: in the STAR magnetic field of 5 kGs, the sagitta of a $P_T = 0.5$ GeV/c track along the path from the vertex to the outer SVT layer (14.4 cm) is just ≃0.8 mm.

As it has already been pointed out, the average SVT occupancy in *pp* mode will be much lower than in the nucleus-nucleus events. Moreover, the average P_T of charged particles generated in the hard *pp* processes of interest will be higher than the mean P_T in heavy ion collisions. These two factors can considerably simplify the direct-track/vertex-finding algorithm for *pp* physics compared to the baseline procedure developed for heavy ions [9, 10]. Schematically, such an algorithm may look as follows[5] (see Figs. 3–6):

1. Take any hit in the outer SVT layer. Draw the plane $\varphi = const$ (plane $P1$ in Fig. 3c) which contains this hit and the central line of the beam, $r = 0$.

2. Draw two more parallel planes, $P2$ and $P3$, at equal distances of ~0.8–1 mm from $P1$ on each of its sides (for illustrative purposes in Figs. 3–6, these distances are chosen to be equal to 1.5 mm, i.e. larger than necessary).

3. Look for hits in the inner and middle layers between planes $P2$ and $P3$ which can potentially belong, along with the chosen hit in the outer layer, to the same high-P_T direct track from the triggered event. The average number of hits within a 2 mm wide strip will be ≤1.5 for the inner layer and ≤1 for the middle layer.

4. Try to draw straight lines in the r–z plane (see Figs. 3–6b) through the chosen hit in the outer barrel and all combinations of the hits in the two other layers which were found in between planes $P2$ and $P3$. Select as the potential candidates for high-P_T tracks just those combinations which satisfy reasonable criteria for belonging to the same straight line. For

[4] The density of the hits from the triggered event shown is higher than the expected average because the displayed SVT section is located around the jet core.

[5] The actual algorithm, while keeping the main points of this scheme, may differ in details.

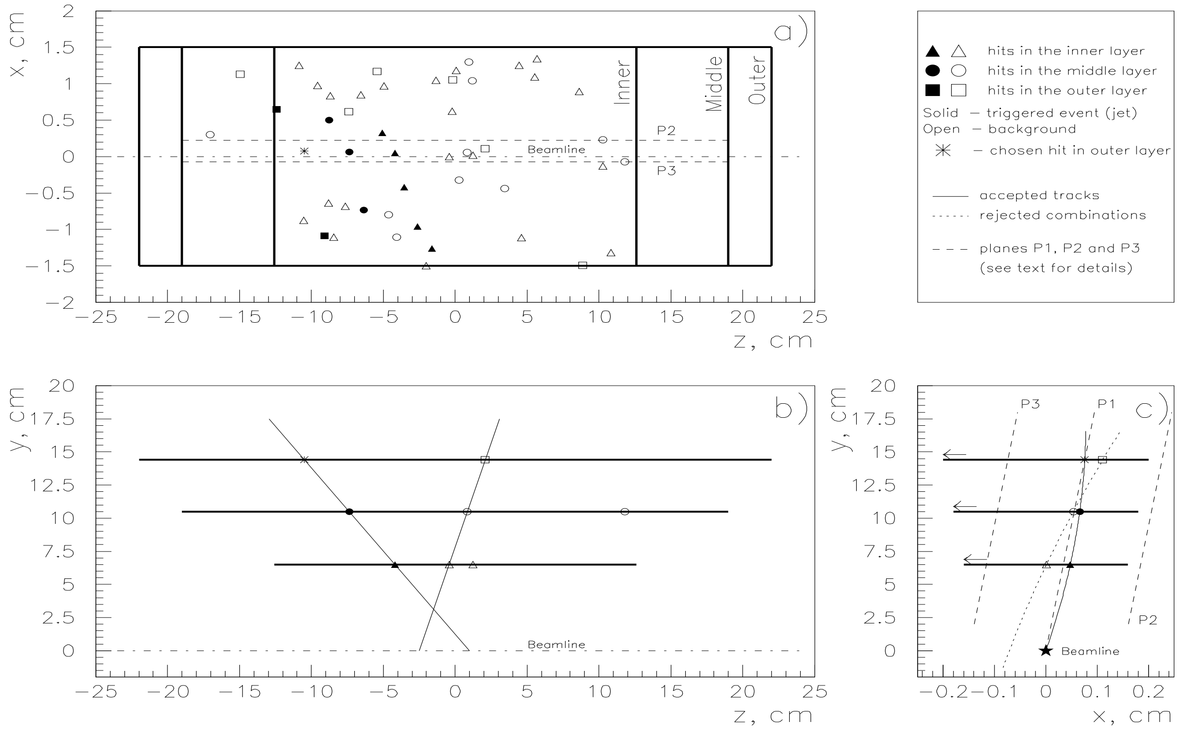

Figure 3: The picture (simplified) of an SVT section with hits from a triggered jet and 120 minimum bias events: **a)** is the "top" view; **b)** is the "side" view of the barrel fractions between planes $P2$ and $P3$; and **c)** is the view along the beam line. All three layers drift in the same direction. The size of the markers has no relation to the SVT position resolution or the pixel size. The shown background track, originating from the bunch crossing 110 ns before the triggered event, passed the Step 4 criteria, but failed at the Step 5.

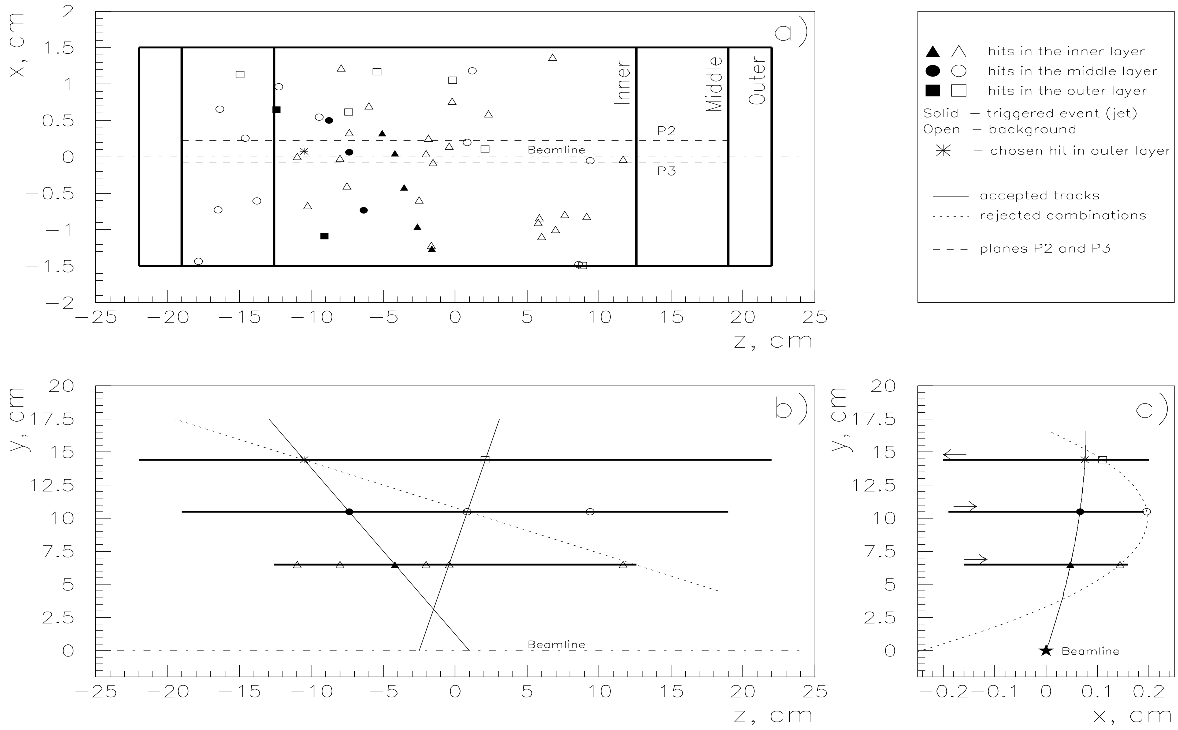

Figure 4: The same as Fig. 3 but with the drift directions reversed in the inner and middle layers.

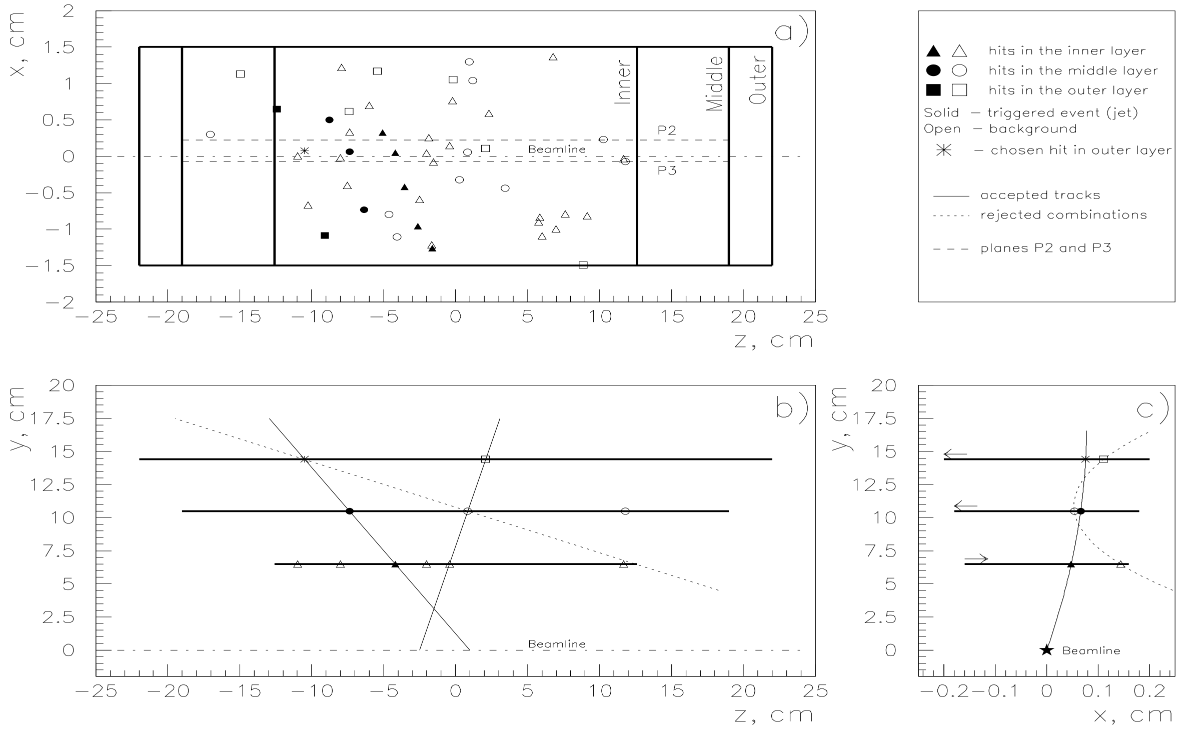

Figure 5: The same as Fig. 3 but with the drift direction reversed in the inner layer.

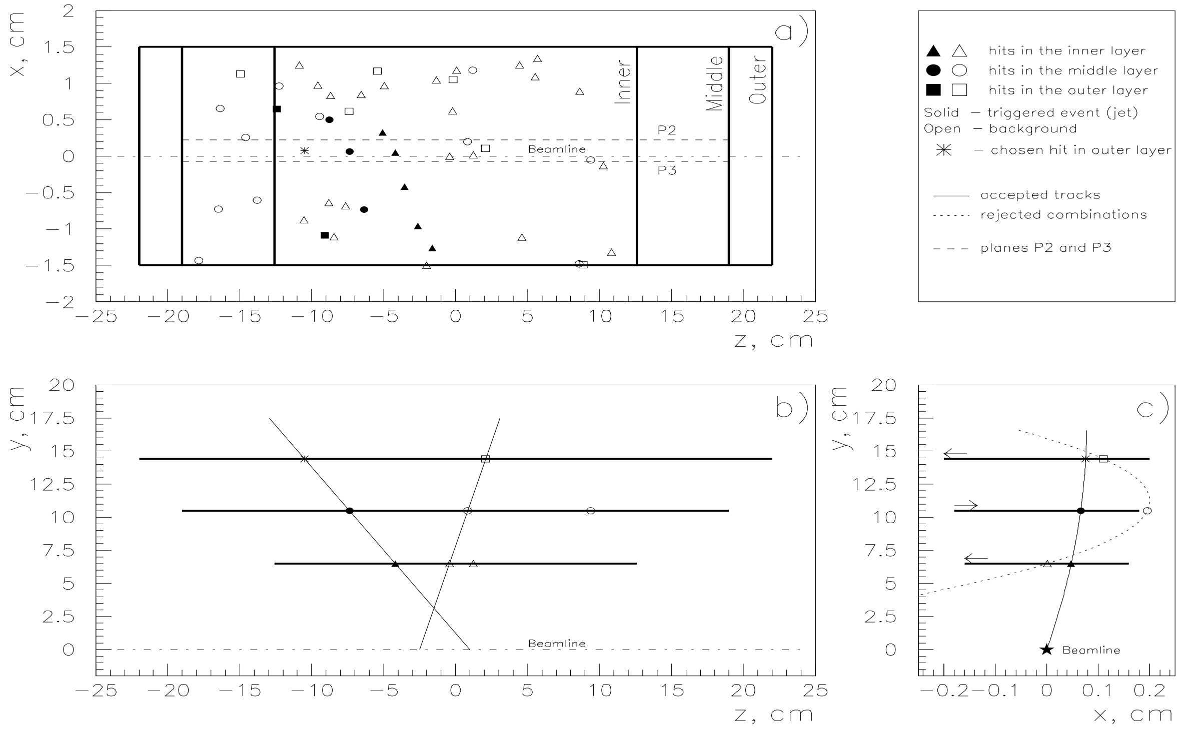

Figure 6: The same as Fig. 3 but with the drift direction reversed in the middle layer.

the occupancy above, there will usually be one or two combinations to try for each hit in the outer layer.

5. In the r–φ plane (Figs. 3–6c), draw circles through all three-hit combinations which passed Step-4. Calculate the impact parameters to the central line of the beam for the reconstructed circles. Select as the direct tracks from the triggered event just those combinations with $P_T \geq P_T^{min}$ which have their impact parameter below a threshold. All other combinations should be rejected as either background or secondary tracks originating from decays.

After Steps 1–4 are repeated for all hits in the outer layer, all "three-hit" high-P_T tracks from the triggered event will be found. However, just a small fraction of the background tracks will be considered for reconstruction. This is because the "measured" φ positions of the hits from events which occur before or after the triggered event will be shifted from the real track crossing points. The shift in azimuth, $\Delta\varphi$, is approximately equal to $-V_{drift} \cdot \Delta t / R_{layer}$, where Δt is the time interval between the trigger and the background event and R_{layer} is the radial position of the SDD. For any particular background track, this provides an additional displacement of the hits in the inner and middle barrels relative to the plane $P1$ drawn through the hit in the outer SDD. This displacement, $\Delta X_{inner/middle}$, is approximately equal to $V_{drift} \cdot \Delta t \cdot (1 \pm R_{inner/middle}/R_{outer})$. The sign in the parenthesis depends on the drift direction in a corresponding layer relative to the drift of the outer hit. For a large Δt, the shift ΔX of the hits in the inner and middle layers will be so large that, at Step 3, they won't even be found between planes $P2$ and $P3$.

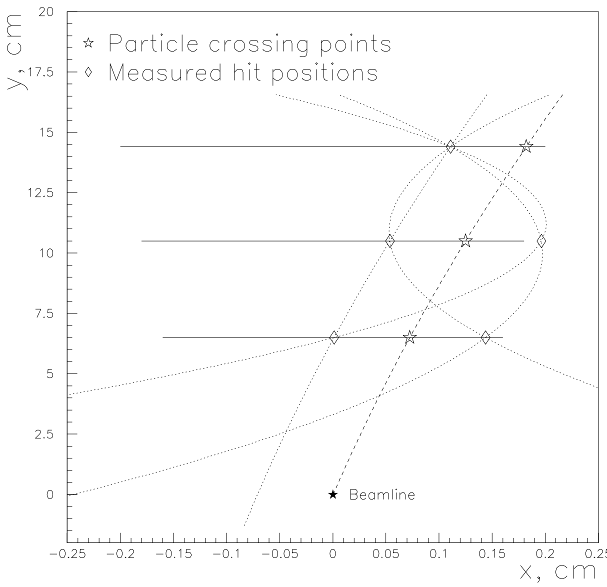

Figure 7: Reconstructing the direct track (r–φ projection) from the bunch crossing, 110 ns before of after the trigger. All four options for the drift directions in the three SVT layers are shown.

Step 5 of the procedure will reject most of the remaining background tracks originating from all bunch crossings except the triggered one. The time interval between crossings, Δt_{min}, in pp mode will be $\simeq$110 ns (114 bunches per each accelerator ring) [2]. Thus, the minimum shift of the "measured" φ positions of the background hits from the actual track crossing points in the SDDs will be equal to $V_{drift} \cdot \Delta t_{min} \simeq 0.7$ mm. There are four, roughly equally probable combinations for the relative drift directions in the SVT layers located at the same azimuth. All these combinations are shown in Fig. 7. If the drifts in all three layers are in the same direction this will result in a shift of the track's r–φ projection, as a whole, by a minimum of $\sim$0.7 mm (see also Fig. 3c). Therefore, the mean impact parameter for these tracks should be expected $\geq$0.7 mm. This is well above the transverse size of the luminous region in pp mode, $\sigma_{rd} \simeq 96$ μm [7]. For the cases with the drifts in the different layers occurring in different directions, the reconstructed impact parameters for background tracks will be even larger (see also Figs. 3–6c).

The distributions of the impact parameters for the "right" crossing and the "wrong" ones, 110 ns before or after the trigger, are shown in Fig. 8a. Apparently, $\sim$3/4 of the tracks from the nearest "wrong" crossings can be separated from the "right" event. The distribution for the remaining $\sim$1/4 (all three hits drift in the same direction) significantly overlaps with the distribution for the "right" tracks. However, for $\Delta t \geq$220 ns, the separation is good enough for the "wrong" tracks to be rejected almost completely (see Fig. 8b).

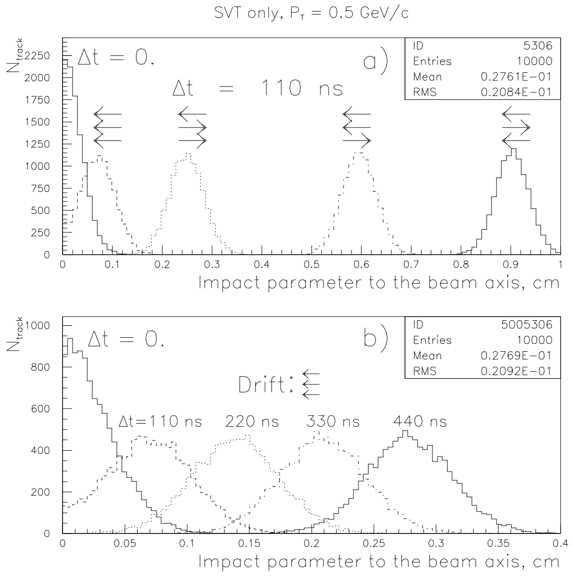

Figure 8: Distributions of the reconstructed impact parameters to the beam axis: **a)** is for $\Delta t = 110$ ns and all four drift options in the SVT layers; **b)** is for the same drift directions in all three layers but various Δt. Statistics are shown for the tracks from the triggered crossing ($\Delta t = 0$).

As a result, at the end of the procedure above, we should expect the following:

- All, $\sim$3–10 high-P_T three-hit direct tracks from the triggered event will be found. They will point to the same z position in the collision diamond with an accuracy of $\sim$200–250 μm. The corresponding distribution is shown in Fig. 9.

- The minimum bias events from three bunch-crossings (the triggered one and the crossings immediately before and after) will contribute $\sim$1–2 more candidates. These tracks will point to different locations within the collision diamond. The probability for two background tracks to point accidentally to the same vertex (within $\sim \pm 0.5$ mm) is on the order of $\sim$1%.

- For the given SDD position resolution and the expected occupancy, the estimated probability for three hits to built up accidentally a straight line in the r–z plane is on the order of $\sim 10^{-4}$. Therefore, after Steps 1–4 are repeated for all $\sim$200–250 hits in the outer layer, the number of "ghost" tracks will be $\sim$0.02–0.03 per trigger. After Step 5, the number of "ghosts" will be reduced to a negligible level of $\sim 10^{-3}$/trigger.

In other words, using the SVT only, the number of candidates for the vertex of the triggered event will be reduced from the initial $\sim$100–120 to $\sim$1–3. Among the remaining vertices, the most probable candidate for the triggered one would be the vertex with the highest multiplicity. The remaining ambiguity, if any, can easily be resolved using the information from other STAR subdetectors.

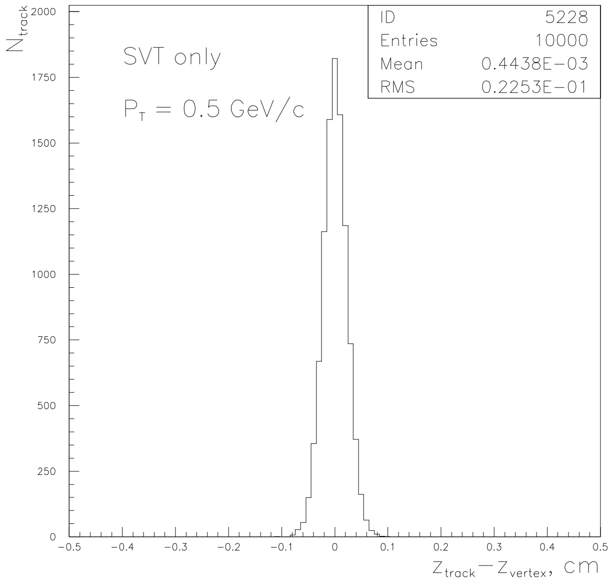

Figure 9: Distribution of the z positions of the track points nearest to the beam axis.

5 Vertex Position and Momentum Resolutions

As soon as all direct high-P_T tracks are found, the vertex position can be reconstructed. In Fig. 10, the distributions of impact parameters to the vertex for high-P_T direct tracks are shown. With the SVT, the impact parameter threshold for the separation of direct and secondary tracks is ∼0.5–0.7 mm, while for the TPC only this threshold is much larger, ∼3–4 mm.

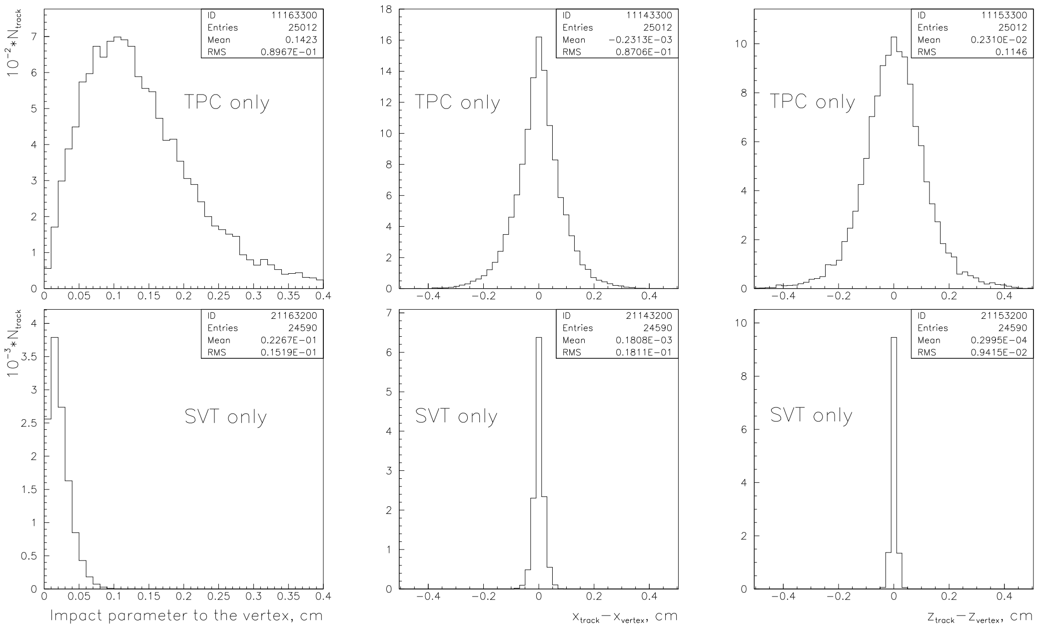

Figure 10: Impact parameters to the vertex for reconstructed high-P_T direct tracks from $pp \to jet + X$ events with $P_T^{jet} \geq 20$ GeV/c. In the left column, the distributions for the three-dimensional distances from the vertex to the nearest points on the tracks are shown. The two other columns are for the projections of these distances onto the axes, perpendicular to the beam (middle), and along the beam (right).

A natural estimate for the vertex location is the point nearest to all direct tracks, $\mathbf{r} = \mathbf{r}_{vtx}^{est}$, where the sum

$$F_1(\mathbf{r}) = \sum_{i=1}^{N_{track}} s_i^2(\mathbf{r})$$

reaches its minimum. In this formula, N_{track} is the number of the found high-P_T direct tracks and $s_i(\mathbf{r})$ is the distance between the i-th track and the point $\mathbf{r}$. The minimization problem for $F_1(\mathbf{r})$ is well defined if there are at least two non-parallel tracks. In Fig. 11, the results of $F_1(\mathbf{r})$ minimization are shown (solid histograms) for 1,000 jet events. The vertex location accuracy, using the SVT, is on the order of 100 μm. With the TPC only it is ~5–7 times worse.

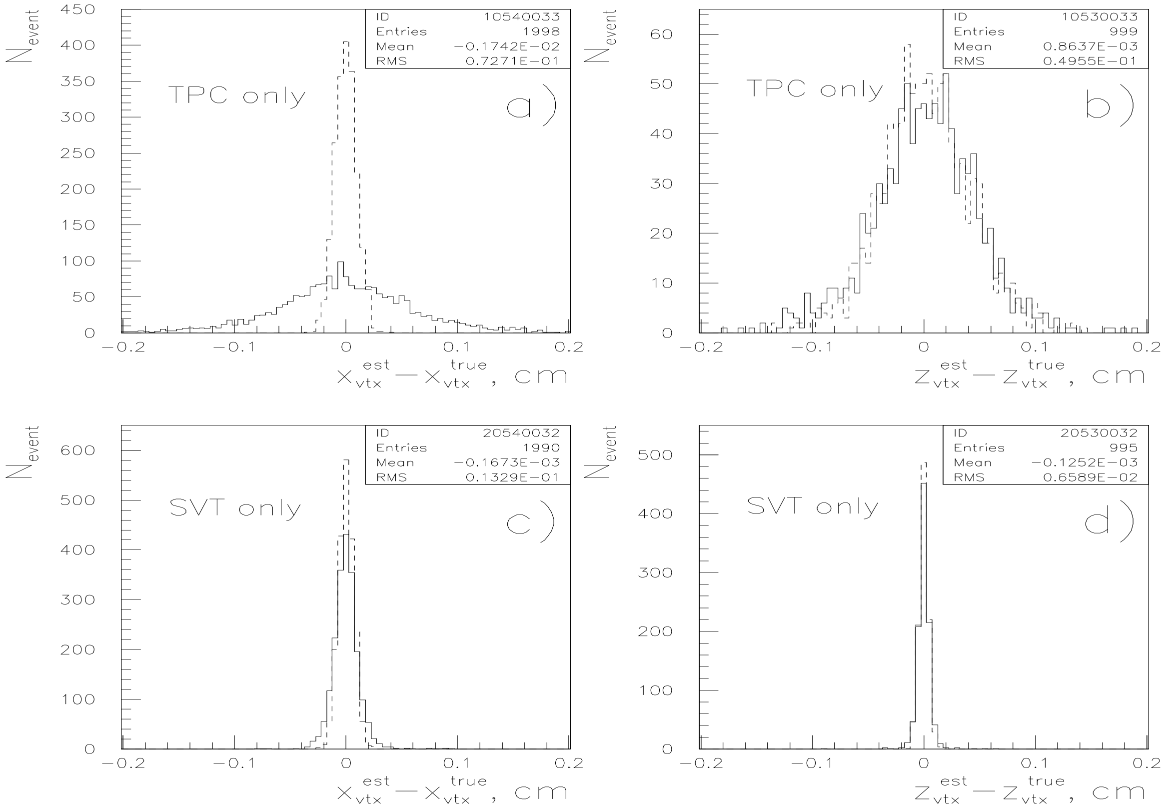

Figure 11: Vertex reconstruction accuracy for $pp \to jet + X$ events with $P_T^{jet} \geq 20$ GeV/c: **a)** and **c)** are for the direction, transverse to the beam; **b)** and **d)** are for the direction along the beam. Solid histograms result from assuming that the size of the collision diamond is unknown (function $F_1(\mathbf{r})$ has been minimized); dashed histograms were obtained, using $F_2(\mathbf{r})$ minimization with $\sigma_{rd} = 96\ \mu m$. Statistics are shown for the solid histograms.

For a known location and size of the collision diamond, the vertex reconstruction accuracy can be improved if, instead of $F_1(\mathbf{r})$, the following function is minimized:

$$F_2(\mathbf{r}) = \frac{F_1(\mathbf{r})}{\sigma_{impact}^2} + \frac{s_0^2(\mathbf{r})}{2\sigma_{rd}^2}$$

where $s_0(\mathbf{r})$ is the distance between the point $\mathbf{r}$ and the central line of the luminous region; σ_{rd} is the transverse size of the collision diamond (96 μm in the *pp* mode; see the footnote in the page 2); and $\sigma_{impact}^2 = $ <(Impact-to-the-vertex)^2> is the mean impact parameter squared of the tracks to the vertex. For the TPC only case, $\sigma_{impact} \simeq$1.7 mm, while for the SVT it is equal to $\simeq$0.3 mm.

The results of the vertex reconstuction using $F_2(\mathbf{r})$ are shown in Fig. 11 as dashed histograms. For the TPC only, the improvement of the transverse vertex resolution is significant: the RMS drops from $\sim$700 μm down to $\sim$95 μm (the size of the luminous region). However, the luminous region constraint does not appreciably affect the resolution along the beam: it changes from the original $\sim$0.5 to just $\sim$0.4 mm. For the SVT with the luminous region constraint, the transverse vertex reconstruction accuracy is $\simeq$70 μm and it is $\simeq$45 μm along the beam.

Simulations in which tracks were reconstructed using the matching hits in both the TPC and the SVT did not show any noticeable improvement of the vertex location accuracy as compared to the SVT only.

In Fig. 12, the simulated high-P_T momentum resolutions in STAR with and without the SVT are shown. While providing just a slight improvement for the direct tracks, the SVT makes a big difference in the P_T resolution for the secondary particles, where the vertex location information cannot be used.

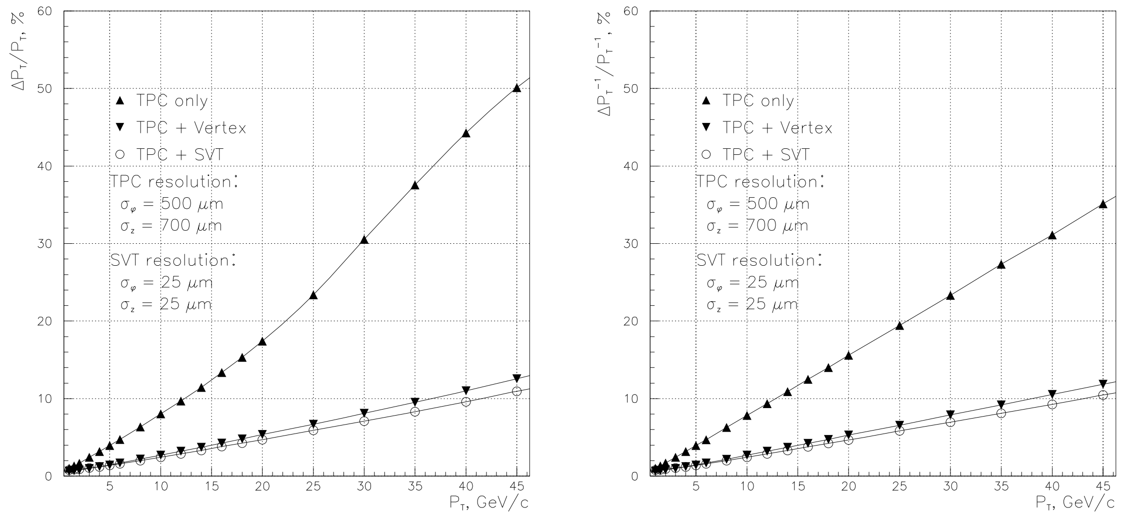

Figure 12: High-P_T momentum resolution (RMS) in STAR.

6 Conclusion

The results of the simulations presented in this paper confirm that the SVT will significantly enhance the STAR detector capabilities for doing high luminosity *pp* physics at RHIC.

With the SVT, the high-P_T direct tracks of the triggered event can easily be selected from the initially stored $\sim$250–300 primarely background tracks which originate from the $\sim$80–100 neighbouring bunch crossings. The number of candidates for the vertex of the triggered event can be reduced to just 1–3, starting from the initial $\sim$100. It is important to underline that these results can be achieved using the SVT alone, without matching information from the TPC and/or other STAR subdetectors. This provides the opportunity to get the job done at the software trigger level.

With the SVT, the vertex location accuracy will be $\sim$50–70 μm, which is $\sim$7–10 times better than $\sim$0.5 mm achievable with only the TPC.

The impact parameter threshold for separating the high-P_T direct and the secondary tracks, originating from short lived particle decays, can be lowered to $\sim$0.5–0.7 mm with the SVT compared to the $\sim$3–4 mm achievable with the TPC alone.

The momentum resolution for high-P_T secondary tracks with the SVT is ~3–5 times better than in the TPC only. The momentum resolution for the direct tracks will also be improved to some degree.

The specifics of the high luminosity *pp* experiment in STAR are very different in many respects from the heavy ion regime. First of all, in the high luminosity *pp* mode it is necessary to reject ≥90–95% of the tracks recorded in the SVT, but even more, ≥99–99.5% of the tracks, stored in the TPC. This problem usually does not exist in the heavy ion experiment at RHIC. The SVT occupancy in *pp* mode will be about 10 times lower than in the TPC. This makes the SVT more attractive than the TPC for the solving the problem of selecting the triggered event.

The SVT occupancy, even at the highest projected *pp* luminosity, will never be more than ~10% of the average occupancy in the central Au-Au events. It is also worth mentionning that, in hard *pp* collision, the average P_T of generated particles will be significantly higher than in heavy ion events. Taking all these differences into account, it makes sense to look into the development of some special tracking algorithms for the SVT in the high luminosity *pp* mode which might be more effective than those developed for heavy ion physics.

7 Acknowledgements

It's my pleasure to thank R. Bellwied, T. M. Cormier, I. V. Kotov, C. A. Pruneau, K. E. Shestermanov, and A. N. Vasiliev for the support and useful discussions, but in particular J. R. Hall and W. K. Wilson for their friendly help at all stages of the preparation of this paper.

References

[1] Conceptual Design Report for the Solenoidal Tracker at RHIC (The STAR Collaboration), BNL, June 15, 1992.

[2] Proposal on Spin Physics Using the RHIC Polarized Collider (RHIC Spin Collaboration), August 1992; Proposal Update, September 1993, and references therein.

[3] E. Gatti and P. Rehak, NIM **A289** (1990) 410.

[4] STAR SVT Requirement Documents, August 1995.

[5] R. Bellwied, et al., Development of Large Linear Silicon Drift Detectors for STAR Experiment at RHIC. Report to the 7th European Symposium on Semiconductor Detectors. Munich, Germany, May 1995 (to be published in NIM).

[6] V. L. Rykov, Reconstructing the Parameters of Charged Particle Hits in the SDD, STAR Note #223, November 1995.

[7] S. White, The Luminous Region, RHIC/DET Note 15, February 1995.

[8] Particle Data Group, Phys. Rev. **D50** (1994) 1335–1336.

[9] D. J. Prindle, SVT Event Reconstruction Algorithms, STAR Note #153, March 1993.

[10] K. Dynowski and C. Pruneau, STAR Note in preparation.

Appendix: Model for Simulations

For the studies presented here, a simplified model of the STAR SVT setup has been used. In this model, three SVT layers of the same thickness, equal to 1% of a radiation length each, are located at the fixed distances from the beam-line, namely, 6.5, 10.5 and 14.4 cm. The helical tracks in the STAR uniform magnetic field $B_z = 5$ kGs have been drawn taking into account small angle multiple scattering (formulas from [8] have been used). Ionization and radiative energy losses have been ignored. The coordinates of the track crossing points for each SDD and TPC layer have been randomly Gaussian smeared with the expected position resolutions (for the SVT, $\sigma_\varphi = \sigma_z = 25\ \mu m$ and, for the TPC, $\sigma_\varphi = 0.5$ mm and $\sigma_z = 0.7$ mm). The layout of the 45 TPC layers corresponds to the TPC geometry defined in the "tpc_pdr.geo" file.

In the track reconstruction procedure, the least squares method has been used. However, at this stage, the layer-to-layer correlations of the hit positions due to multiple scattering have been ignored.